In-Plane and Out-of-Plane Optical Spectra of Sr_2RuO_4

T. Katsufuji,[1] M. Kasai,[2] and Y. Tokura[1,2]
[1]*Department of Applied Physics, University of Tokyo, Tokyo 113, Japan*
[2]*Joint Research Center for Atom Technology (JRCAT), Tsukuba 305, Japan*
(Received 17 July 1995)

In-plane (ab-plane) and out-of-plane (c-axis) optical spectra were investigated at various temperatures for Sr_2RuO_4 which is isostructural with the cuprate superconductor $La_{2-x}Sr_xCuO_4$ and becomes superconducting below 1 K. The ratio of the in-plane to out-of-plane low-energy spectral weight of this compound is approximately 10^2, an anisotropy comparable to that of the cuprate. The temperature dependence of the c-axis spectrum suggests coherent motion of conduction carriers with strongly renormalized mass and scattering rate along the c axis at low temperatures.

PACS numbers: 74.25.Gz, 74.70.Ad, 78.30.Er

One of the characteristic properties in the high-T_c cuprate superconductors is anisotropic charge dynamics in the normal state [1]. In-plane resistivity (ρ_{ab}) and interplane resistivity (ρ_c) show different temperature dependence above T_c in the lightly doped region: ρ_{ab} decreases with lowering temperature whereas ρ_c increases such as in semiconductors. The temperature dependence of ρ_c is sensitive to the doping level, and $d\rho_c/dT$ turns positive in the heavily doped region. Several optical studies about the interplane charge dynamics [2–6] have also been carried out and revealed that c-axis optical conductivity spectrum in the normal state shows no sharp Drude peak at $\omega \sim 0$ but a gradual decrease (or a nearly constant value) in intensity with an increase of ω, which is reminiscent of a dirty metal. On the other hand, in the superconducting state the low-energy ($<$0.02 eV) spectral weight is condensed to $\hbar\omega \sim 0$ eV, which yields a sharp plasma edge in the c-axis far-infrared reflectivity spectrum.

Recently, Sr_2RuO_4 with K_2NiF_4 structure was found to become superconducting below $\sim$1 K [7]. Since this compound is nearly isostructural with $La_{2-x}Sr_xCuO_4$ (apart from the orthorhombic distortion of the cuprate), a comparison of the interplane charge dynamics in the normal state between Sr_2RuO_4 and the cuprates will be helpful to comprehend the anisotropic charge dynamics in strongly correlated metals as well as to distinguish characteristic properties in the cuprates. According to resistivity measurements on Sr_2RuO_4 single crystals [7–9], ρ_{ab} decreases with a decrease of temperature, whereas ρ_c is nearly temperature independent above 130 K and shows a rapid decrease with a decrease of temperature below 130 K. The magnetic susceptibility above T_c is nearly temperature independent [7], which is characteristic of a typical paramagnetic metal. However, the effect of electron correlation is likely to play an important role in the low-energy electronic structure and charge dynamics in Sr_2RuO_4, as evidenced, for example, by experimental observations of an enhanced electronic specific-heat coefficient and Pauli paramagnetic susceptibility [7] and a narrowed dispersion of the conduction band [10]. In this Letter, in-plane (ab-plane) and out-of-plane (c-axis) optical spectra of a Sr_2RuO_4 single crystal are reported at various temperatures together with their analysis. The result indicates that the electronic structure of Sr_2RuO_4 is comparably anisotropic to that of cuprates, but the interplane charge dynamics is qualitatively different between Sr_2RuO_4 and cuprates: In the former compound the c-axis transport is governed by the coherent motion of charge carriers with strongly renormalized mass and scattering rate in contrast to the incoherent nature of the c-axis transport in the normal state of the cuprates.

The single crystal investigated in this study was grown by the floating-zone method. $SrCO_3$ and RuO_2 in the molar ratio 2:1.1 were prereacted in air, pressed into a rod, and then loaded in a floating-zone furnace. A single crystal was melt grown from this rod in air with a feeding speed of 20 mm/h. The grown crystal was easily cleaved along the growth direction with the (001) surface (as determined by the x-ray Laue diffraction), and a typical size of the specimen is 6 mm $\times$ 6 mm $\times$ 2 mm. We cut it perpendicularly to the (001) surface, and prepared the (101) plane which was polished to the optical flatness. Reflectivity measurements at room temperature were carried out on the (101) surface between 0.008 eV and 40 eV for $\mathbf{E} \perp \mathbf{c}$ (in plane) and $\mathbf{E} \parallel \mathbf{c}$ (interplane) polarizations, using a Fourier-transform interferometer (0.008–0.8 eV) and grating spectrometers (0.6–40 eV) with the use of appropriate polarizers. Synchrotron radiation at INS-SOR, University of Tokyo, was utilized for the measurements between 6 and 36 eV. Measurements at low temperatures were carried out using a temperature-variable cryostat between 0.008 and 0.08 eV for $\mathbf{E} \parallel \mathbf{c}$ and between 0.06 and 3 eV for $\mathbf{E} \perp \mathbf{c}$. [However, we could not make the measurement of the superconducting state owing to the low T_c ($\sim$0.9 K).] Optical response functions were obtained by Kramers-Kronig analysis of the reflectivity data at each temperature that was extrapolated with the room-temperature data for the higher energy region.

Figure 1 shows spectra of (a) reflectivity $R(\omega)$ and (b) optical conductivity $\sigma(\omega)$ for both polarizations. Spectra for $\mathbf{E} \perp \mathbf{c}$ polarization (in plane) at 290 and 9 K are Drude-like; namely, $R(\omega)$ sharply increases towards $R = 1$ below $\sim$1.7 eV, and $\sigma(\omega)$ shows the maximum

 0031-9007/96/76(1)/126(4)$06.00

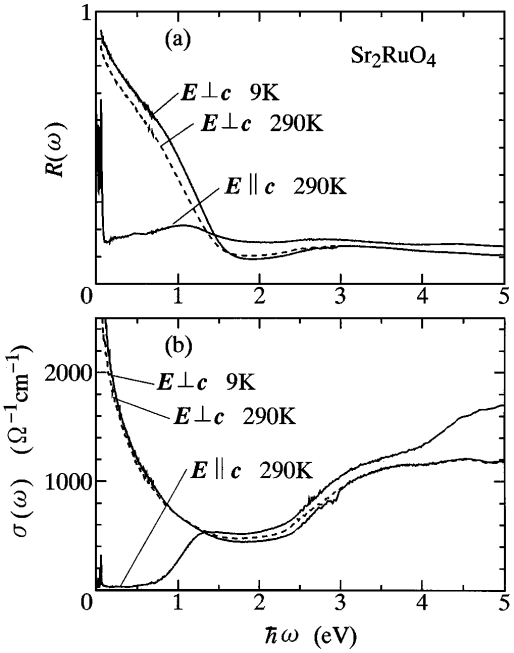

FIG. 1. (a) Reflectivity $R(\omega)$ and (b) optical conductivity $\sigma(\omega)$ spectra below 5 eV for $\mathbf{E} \perp \mathbf{c}$ at 290 K (dashed line) and 9 K (solid line), and for $\mathbf{E} \parallel \mathbf{c}$ at 290 K.

at $\hbar\omega = 0$ eV. $R(\omega)$ is higher at 9 K than at 290 K for $\hbar\omega < 1.5$ eV, and $\sigma(\omega)$ is higher at 9 K than at 290 K at $\hbar\omega \sim 0$ eV, which is consistent with the temperature dependence of dc resistivity [7–9]. On the other hand, the spectrum for $\mathbf{E} \parallel \mathbf{c}$ (out of plane) at 290 K is quite different from the in-plane spectra: $R(\omega)$ does not show a Drude-like feature in the low energy region, and $\sigma(\omega)$ shows nearly $\hbar\omega$-independent spectra below 0.5 eV (apart from the sharp phonon structures below 0.1 eV) whose magnitude is much smaller than that for $\mathbf{E} \perp \mathbf{c}$. Such a c-axis spectrum is similar to those of cuprate superconductors, e.g., $YBaCu_{23}O_{7-\delta}$ [2–4] and $La_{2-x}Sr_xCuO_4$ [5,6], in the normal state.

To estimate the Drude weight, we calculated the effective number of electrons, $N_{\mathrm{eff}}(\omega) = (2m_0/\pi e^2 N)\int_0^{\omega} \sigma(\omega')d\omega'$, where m_0 is the free electron mass and N the number of Ru atoms per unit volume. In the simple Drude model [$\sigma(\omega) = ne^2\tau/m(1 + \omega^2\tau^2)$, where n, m, and τ are the number of carriers per unit volume, the carrier mass, and the relaxation time of carriers, respectively], $N_{\mathrm{eff}}(\omega \to \infty)$ is $(n/N)/(m/m_0)$. In the case where the spectrum for an interband transition is superposed, however, the upper limit of the $\sigma(\omega)$ integral should be taken below the onset energy of the interband transition, but sufficiently higher than τ^{-1} (inversed relaxation time) to extract only the Drude part. We thus examined the value of $N_{\mathrm{eff}}(\omega)$ at $\hbar\omega = 1.5$ eV for $\mathbf{E} \perp \mathbf{c}$ and 0.5 eV for $\mathbf{E} \parallel \mathbf{c}$, and found that the in-plane effective number of electrons for conduction carriers (N_{eff}^{ab}) is ~0.53, and the interplane one (N_{eff}^{c}) is ~0.007. The anisotropic ratio $N_{\mathrm{eff}}^{ab}/N_{\mathrm{eff}}^{c}$ is ~80, which is comparably large to that of $La_{2-x}Sr_xCuO_4$ in the heavily doped region (e.g., at $x = 0.30$) [6]. According to the local density approximation band calculation of $\mathbf{Sr_2}RuO_4$ [11], N_{eff}^{ab} and N_{eff}^{c} are 1.4 and 0.011, respectively [12]. The absolute values of N_{eff}^{ab} and N_{eff}^{c} estimated by the band calculation are approximately twice as large as the experimental ones, respectively, indicating that the effective mass (optical mass) of the conduction carriers of this compound is about twice the calculated one. Nevertheless, the anisotropy of the low-energy electronic structures ($N_{\mathrm{eff}}^{ab}/N_{\mathrm{eff}}^{c}$) is rather correctly evaluated by the LDA calculation.

The spectrum for $\mathbf{E} \parallel \mathbf{c}$ shows a conspicuous change with temperature in the far-infrared region. Figure 2 shows spectra of (a) $R(\omega)$ and (b) $\sigma(\omega)$ for $\mathbf{E} \parallel \mathbf{c}$ at various temperatures below 0.05 eV. The spectrum at 130 K is nearly the same as that at 290 K, except for the sharpening of three phonon structures at 0.025, 0.045, and 0.06 eV (the last one is not seen in Fig. 2. Below 130 K, $R(\omega)$ in between 0.01 and 0.02 eV decreases whereas that below 0.01 eV increases, forming a Drude-like spectrum. The dashed lines in the $R(\omega)$ spectra represent the extrapolation by the simple Drude form, $R(\omega) = |[\sqrt{\epsilon(\omega)} - 1]/[\sqrt{\epsilon(\omega)} + 1]|^2$, where $\epsilon(\omega) = \epsilon_\infty - \omega_p^2/\omega(\omega + i/\tau)$. In this functional form, there are three variable parameters: ω_p, τ, and ϵ_∞. We fixed the ϵ_∞ value at 10 [13], and chose ω_p and τ so that both the calculated absolute value and the derivative of the Drude-model spectrum become identical to those of the experimental spectrum at 0.007 eV. The $\sigma(\omega)$ spectra shown in Fig. 2(b) are obtained by

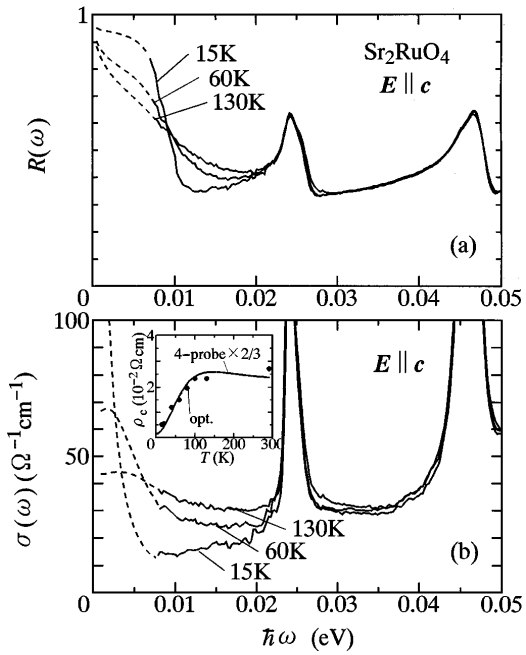

FIG. 2. (a) Reflectivity $R(\omega)$ and (b) optical conductivity $\sigma(\omega)$ spectra below 0.05 eV for $\mathbf{E} \parallel \mathbf{c}$ at 130, 60, and 15 K. Dashed lines are the extrapolation by the Drude function (see text). The inset of (b) shows a comparison of the optically deduced c-axis resistivity ($\rho_c = [\sigma(\omega = 0\ \mathrm{eV})]^{-1}$) with that measured by the conventional four-probe technique, which is multiplied by 2/3.

the Kramers-Kronig transformations of extrapolated reflectivity spectra. Dashed-line parts ($\hbar\omega < 0.007$ eV) in Fig. 2 are thus rather qualitative, yet the temperature dependence of $\sigma(\omega = 0\ \text{eV})$ is in good agreement with the dc conductivity obtained by the conventional four-probe technique as indicated in the inset of Fig. 2(b). We also made other types of low-energy extrapolation, i.e., Hagen-Rubens ($R = 1 - c\omega^{1/2}$) and constant extrapolation for $\hbar\omega < 0.007$ eV, and confirmed that variation in $\sigma(\omega)$ above 0.007 eV with the three different types of extrapolation is $< 5\%$. As can be seen in Fig. 2(b), the spectral weight of $\sigma(\omega)$ between 0.005 and 0.03 eV is diminished and is condensed to $\hbar\omega \sim 0$ eV with a decrease of temperature below 130 K, which corresponds to the rapid decrease of dc resistivity in this temperature range. It is noteworthy that the effective number of electrons $[N_{\text{eff}}(\omega)]$ is nearly conserved at $\hbar\omega \sim 0.03$ eV under variation of temperature.

In the case of high-T_c cuprate superconductors, the temperature dependence of the optical spectra for $\mathbf{E} \parallel \mathbf{c}$ varies with doping: For the compound located in the lightly doped region, e.g., $YBa_2Cu_3O_{6.7}$ [3], the low-energy spectral weight (< 0.03 eV) is diminished with a decrease of temperature above T_c. However, this missing spectral weight is not condensed to $\hbar\omega \sim 0$ eV but redistributed over the higher energy region, which is consistent with the insulating behavior of the c-axis conduction, i.e., $d\rho/dT < 0$. On the other hand, for the compound located in the heavily doped region $YBa_2Cu_3O_7$ [4], for example), $\sigma(\omega = 0\ \text{eV})$ increases with a decrease of temperature (i.e., $d\rho/dT > 0$), which is qualitatively similar to the case of Sr_2RuO_4 below 130 K. For the cuprate, however, $\sigma(\omega)$ increases rather uniformly for $\hbar\omega < 0.1$ eV with a decrease of temperature [4], and this makes a sharp contrast to the case of Sr_2RuO_4, where $\sigma(\omega)$ between $\omega = 0.005$ and 0.03 eV decreases, whereas that below 0.005 eV increases, conserving the total spectral weight below 0.3 eV. Such a condensation of the spectral weight of $\sigma(\omega)$ to $\hbar\omega \sim 0$ eV is observed only for the cuprates below T_c [3–5], where the conduction carrier can move coherently as the Cooper pairs along the c axis.

To interpret the c-axis optical spectra shown in Fig. 2 in a more quantitative manner, we made the extended Drude analysis [14], in which optical response function is expressed as

$$\sigma(\omega) = \frac{\omega_p^2}{4\pi} \frac{\tau(\omega)}{1 + [m^*(\omega)/m]^2\omega^2\tau(\omega)^2},$$

$$\epsilon_1(\omega) = \epsilon_\infty - \omega_p^2 \frac{[m^*(\omega)/m]\tau(\omega)^2}{1 + [m^*(\omega)/m]^2\omega^2\tau(\omega)^2}. \quad (1)$$

Here $m^*(\omega)$ and $\tau(\omega)$ are the energy-dependent mass and relaxation time of the conduction carriers, m the unrenormalized mass, and ω_p (unrenormalized plasma frequency) $= \sqrt{4\pi ne^2/m}$, where n is the density of carriers. We determined the c-axis plasma frequency ω_p^c to be 0.32 eV, which corresponds to the magnitude of the c-axis effective number of electrons ($N_{\text{eff}}^c = 0.007$). In the extended Drude analysis, $m^*(\omega)/m$ and $\tau(\omega)$ are obtained by the $\sigma(\omega)$ and $\epsilon_1(\omega)$ (not shown) spectra from which phonon structures are subtracted. Figure 3 shows the ω dependence of the c-axis mass and scattering rate; (a) $m_c^*(\omega)/m_c$ and (b) $\hbar/\tau_c(\omega)$. The ω dependence of m_c^* and $\hbar/\tau_c$ is rather small at 130 K. Since the magnitude of $\hbar/\tau_c$ (~ 0.25 eV) is comparably large to that of ω_p^c ($= 0.32$ eV), Sr_2RuO_4 may be viewed as a dirty metal at (and above) 130 K. Below 130 K, m_c^* for $\hbar\omega < 0.02$ eV is enhanced and reaches about 30 times the unrenormalized c-axis mass m_c for $\hbar\omega < 0.01$ eV at 15 K. (Note that m_c itself is readily about 10^2 as large as the ab-plane mass m_{ab}.) On the other hand, $\hbar/\tau_c$ is suppressed for $\hbar\omega < 0.012$ eV whereas it increases for $\hbar\omega > 0.012$ eV with the decrease of temperature. Such features can be interpreted in terms of the onset of the coherent motion of the carriers along the c axis whose interplane effective mass is highly enhanced through the low-energy renormalization. It should be noted that temperature dependence of $m_c^*(\omega)/m$ and $\hbar/\tau_c(\omega)$ of Sr_2RuO_4 below 130 K is similar to that of a heavy fermion compound URu_2Si_2 below 70 K [15]. In URu_2Si_2, resistivity reaches the maximum at 70 K and shows rapid decrease below this temperature (in the coherent regime), which is analogous to the c axis transport of Sr_2RuO_4 [16].

For comparison, we also applied the extended Drude analysis to the spectra for $\mathbf{E} \perp \mathbf{c}$ (in-plane spectra). As seen in Fig. 4, $m_{ab}^*(\omega)/m$ is nearly independent of $\hbar\omega$ and temperature (T), though a small mass enhancement is observed in a temperature-dependent manner below 0.3 eV with the decrease of T. On the other hand, $\hbar/\tau_{ab}$ shows a nearly ω-independent decrease with the

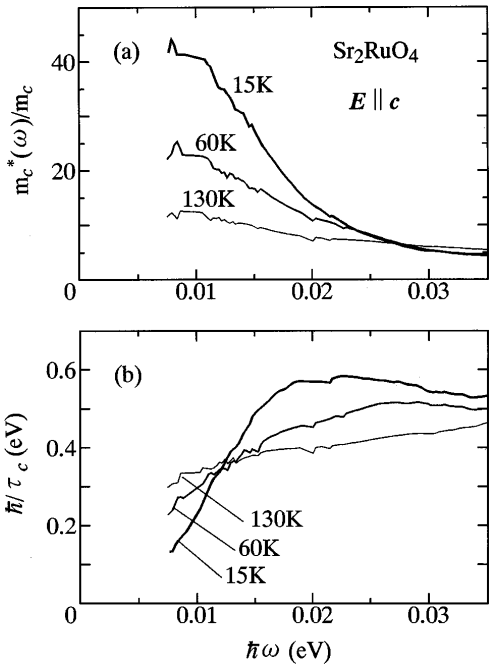

FIG. 3. (a) Energy-dependent effective mass divided by the unrenormalized mass $[m_c^*(\omega)/m_c]$ and (b) the scattering rate $[\hbar/\tau_c(\omega)]$ for $\mathbf{E} \parallel \mathbf{c}$ at 130, 60, and 15 K.

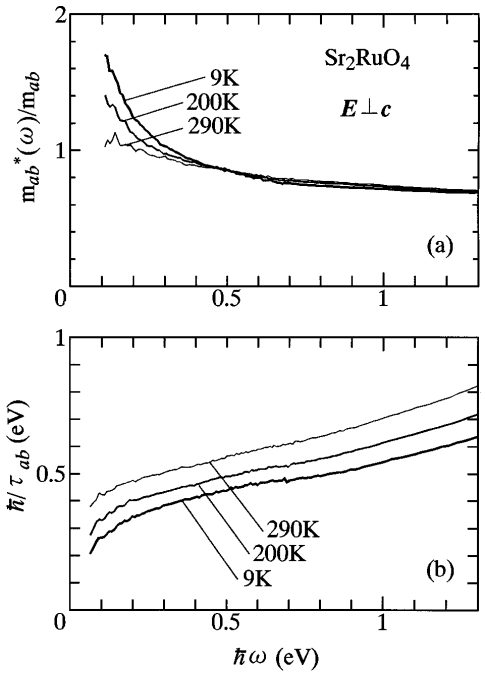

FIG. 4. (a) Energy-dependent effective mass divided by the unrenormalized mass $[m^*_{ab}(\omega)/m_{ab}]$ and (b) the scattering rate $[\hbar/\tau_{ab}(\omega)]$ for $\mathbf{E} \perp \mathbf{c}$ at 290, 200, and 9 K.

decrease of T. In the simplest Fermi liquid theory [17], m^* is a constant value against ω and T, and $1/\tau$ is given by $1/\tau(\omega, T) = 1/\tau_0 + 1/\tau(\omega) + 1/\tau(T)$, where $1/\tau_0$ is for the impurity scattering. Such a separation in the ω and T dependence of $1/\tau$ will lead to the rigid shift of $1/\tau(\omega)$ under variation of T, which is in accord with the presently observed feature for the $\mathbf{E} \perp \mathbf{c}$ spectra. It is also derived from the Fermi liquid theory that $1/\tau(\omega)$ and $1/\tau(T)$ are proportional to ω^2 and T^2, respectively, for sufficiently low ω and T, the latter of which is responsible for the T^2 law of the resistivity ($\rho = \rho_0 + AT^2$). In this compound $\rho_{ab}(T)$ obeys T^2 law at least below 100 K [7,9]. We estimated the T^2 coefficient (A) from $1/\tau_{ab}(T)$ (magnitude of the shift of $1/\tau_{ab}(\omega)$ with T) and ω_p^{ab} (plasma frequency derived by N_{eff}^{ab}) with use of the relation $\rho_{ab}(T) = 4\pi/[\omega_p^{ab}]^2\tau_{ab}(T)$, and thus found that the estimated value of A corresponds well to that determined from the dc resistivity measurement [9] within an error of factor two. Thus, the observed $\hbar\omega$ and T dependence of m^*_{ab} and $\hbar/\tau_{ab}$ for $\mathbf{E} \perp \mathbf{c}$ preserve the features of conventional Fermi liquid metals. Incidentally, ω^2 dependence of $1/\tau_{ab}$ is not observable in Fig. 3(b), and would show up only in the much lower energy region than the energy scale of room temperature ($\sim$0.03 eV).

In summary, ab-plane (in-plane) and c-axis (out-of-plane) optical spectra of Sr_2RuO_4 were investigated at various temperatures. Anisotropy of the low-energy spectral weight ($\sim 10^2$) is comparably large to that of cuprates. The ω and T dependence of ab-plane spectra ($\mathbf{E} \perp \mathbf{c}$) is consistent with that of normal metals. However, the spectral weight of $\sigma(\omega)$ for $\mathbf{E} \parallel \mathbf{c}$ between 0.005 and 0.03 eV begins to be condensed to $\hbar\omega \sim 0$ eV when the temperature is lowered below 130 K, which is different from the behavior of cuprates in the normal state. The extended Drude analysis of the c-axis spectrum suggests the onset of the coherent motion of carriers with strongly renormalized mass and scattering rate along the c axis below 130 K. Such an anisotropic renormalization effect in the charge dynamics may be considered as a generic feature of the quasi-two-dimensional metal with strong electron correlation, but is obviously distinct from the case of the cuprate superconductors.

We are grateful to Y. Okimoto and T. Ishikawa for their collaboration in setting up the experimental system. We also thank T. Yokoya and T. Takahashi for enlightening discussions. The present work was supported by a Grant-In-Aid for Scientific Research from the Ministry of Education, Science, and Culture, Japan, and also by the New Energy and Industrial Technology Development Organization (NEDO) of Japan.

[1] T. Ito, H. Takagi, S. Ishibashi, T. Ido, and S. Uchida, Nature (London) **350**, 596 (1991); Y. Nakamura and S. Uchida, Phys. Rev. B **47**, 8369 (1993); T. Takenaka, K. Mizuhashi, H. Takagi, and S. Uchida, Phys. Rev. B **50**, 6534 (1994).
[2] S. L. Cooper *et al.*, Phys. Rev. B **47**, 8233 (1993).
[3] C. C. Homes, T. Timusk, R. Liang, D. A. Bonn, and W. N. Hardy, Phys. Rev. Lett. **71**, 1645 (1993).
[4] J. Schützmann, S. Tajima, S. Miyamoto, and S. Tanaka, Phys. Rev. Lett. **73**, 174 (1994).
[5] K. Tamasaku, Y. Nakamura, and S. Uchida, Phys. Rev. Lett. **69**, 1455 (1992).
[6] K. Tamasaku, T. Ito, H. Takagi, and S. Uchida, Phys. Rev. Lett. **72**, 3088 (1994).
[7] Y. Maeno, H. Hashimoto, K. Yoshida, S. Nishizaki, T. Fujita, J. G. Bednorz, and F. Lichtenberg, Nature (London) **372**, 532 (1994).
[8] F. Lichtenberg, A. Catana, J. Mannhart, and D. G. Schlom, Appl. Phys. Lett. **60**, 1138 (1992).
[9] M. Kasai and Y. Tokura (unpublished).
[10] T. Yokoya, A. Chainani, T. Takahashi, H. Karayam-Yoshida, M. Kasai, and Y. Tokura (to be published).
[11] T. Oguchi, Phys. Rev. B **51**, 1385 (1995).
[12] We derived these values from the plasma frequency ω_p shown in Ref. [11], with the relation $\omega_p^2 = 4\pi N_{\text{eff}} Ne^2/m_0$.
[13] The value at 0.008 eV (sufficiently below the lowest frequency phonon) of $\epsilon_1(\omega)$ at 290 K, which was derived by the Kramers-Kronig transformation of the reflectivity with constant extrapolation in the lower energy region.
[14] J. W. Allen and J. C. Mikkelsen, Phys. Rev. B **15**, 2952 (1977).
[15] D. A. Bonn, J. D. Garrett, and T. Timusk, Phys. Rev. Lett. **61**, 1305 (1988).
[16] Another possible way to analyze the c-axis spectra would be on the basis of the two-component model, proposed by A. G. Rojo and K. Levin [Phys. Rev. B **48**, 16 861 (1993)].
[17] D. Pines and P. Nozieres, *The Theory of Quantum Liquids* (Benjamin, New York, 1966).